JBC Papers in Press. Published on September 21, 2011 as Manuscript M111.287268
The latest version is at http://www.jbc.org/cgi/doi/10.1074/jbc.M111.287268

A novel degradation signal derived from distal C-terminal frame-shift mutations of KCNQ2 which cause neonatal epilepsy

Jun Su[1], Xu Cao[1] and KeWei Wang[1,2¶]

[1]Department of Neurobiology, Neuroscience Research Institute, Peking University Health Science Center; [2]Department of Molecular and Cellular Pharmacology, Peking University School of Pharmaceutical Sciences, 38 Xueyuan Road, Beijing 100191, China

Running title: Accelerated degradation signal of KCNQ2 mutation

[¶] To whom correspondence should be addressed:
KeWei Wang, MD., PhD.
Professor of Neurobiology
Peking University School of Medicine
38 Xueyuan Road, Beijing 100091
wangkw@bjmu.edu.cn
Tel: (8610) 82805065
Fax: (8610) 82805065

Key words: BFNC, epilepsy, ubiquitin, proteasome, protein degradation

Capsule:
Background: The mechanism underlying incomplete dominance of KCNQ2 channel mutations which cause epilepsy remains unknown.
Results: We have identified a novel degradation signal with a key five-amino acid (RCXRG) motif from distal C-terminal frame-shift mutations of KCNQ2.
Conclusion: The novel degradation signal accelerates degradation of surface mutant proteins through ubiquitin-independent proteasome machinery.
Significance: Our findings reveal a mechanism by which mutant KCNQ2 proteins cause epilepsy.

Benign familial neonatal convulsions (BFNC) is an autosomal-dominant idiopathic form of epilepsy primarily caused by gene mutations of the voltage-gated Kv7.2/KCNQ2/M-channel which exert only partial dominant-negative effects. However, the mechanism underlying the incomplete dominance of channel mutations which cause epilepsy in infancy remains unknown. Using mutagenesis and biochemistry combined with electrophysiology, we identified a novel degradation signal derived from distal C-terminal frame-shift mutations which impairs channel function. This degradation signal, transferable to non-channel CD4, can lead to accelerated degradation of mutant proteins through ubiquitin-independent proteasome machinery, but does not affect mRNA quantity and protein trafficking. Functional dissection of this signal has revealed a key five-amino acid (RCXRG) motif critical for degradation. Taken together, our findings reveal a mechanism by which proteins that carry this signal are subject to degradation, leading to M-current dysfunction which causes epilepsy.

Benign familial neonatal convulsions (BFNC) is an autosomal-dominant form of idiopathic epilepsy, characterized by unprovoked partial or generalized seizures within a week after birth and remission after 3-10 weeks (1). In most patients psychomotor development is normal, but about 15% individuals suffer from seizures later in life (2,3). BFNC is caused by mutations in voltage-gated Kv7.2/KCNQ2 or Kv7.3/KCNQ3 potassium channel genes which encode a low threshold, non-inactivating native M-current (4-7). M-current regulates neuronal excitability, and inhibition of M-current or loss-of-function of KCNQ2 leads to repetitive firing and epileptic seizures in mice (8,9). Most known BFNC mutations have been identified in KCNQ2, but a few reside in KCNQ3 (10). Among the KCNQ2 mutations that have been tested, none exert complete dominant-negative effects on wild-type KCNQ2 (6,11,12). These observations have lead to the conclusion that BFNC is caused by haploinsufficiency, indicating that the single functional copy of the KCNQ2 gene in BFNC patients does not produce enough functional channel protein.

Kv7.2/KCNQ2 is a member of the Kv7 family, and has six transmembrane domains followed by a long cytoplasmic C-terminus that contains many functional motifs and domains. It has previously been shown that most BFNC mutations located in the C-terminus of KCNQ2 (6,13), including two distal C-terminal frame-shift mutations of KCNQ2, Q2-*2513del1bp* (one nucleotide deletion at 2513 bp), and Q2-*2516ins5bp* (5 nucleotide insertion at 2516 bp) in which there is substitution of only the last 7 or 2 residues respectively. These two distal C-terminal frame-shift mutations exhibit normal biophysical properties, but show reduced current density (13-15). However, the clinical phenotype of epileptic patients carrying these two distal C-terminal frame-shift mutations is no less serious than that in patients

with loss-of-function mutations in the pore region that functions as the channel gate and ion selectivity filter (13,14,16). This raises questions as to how the two distal C-terminal frame-shift mutations impair channel function and cause epilepsy.

Protein degradation is highly selective with individual protein half-lives ranging from minutes to years (17). A degradation signal is defined as a protein sequence that can reduce the half-life of the target protein and is sufficient for recognition and degradation by distinct proteolytic pathways (17,18). An important property of degradation signals is their transferability, and genetically engineered attachment of such signal sequences leads to metabolic instability in otherwise long-lived proteins (17).

In this study, we investigated the mechanism by which two C-terminal frame-shift mutations which bring about the impairment of the channel function that underlies BFNC. Using biochemical approaches combined with electrophysiology, we identified a novel degradation signal in the extended segments of the two frame-shift mutations. This degradation signal contains a critical five-amino acid motif, which leads to accelerated degradation of the mutant proteins through the ubiquitin-independent proteasome machinery, but does not affect mRNA quantity and protein trafficking. Our findings demonstrate that BFNC haploinsufficiency is caused by accelerated degradation of channel proteins carrying the degradation signal, and this cellular mechanism brings about impaired channel function and causes neonatal epilepsy.

EXPERIMENTAL PROCEDURES

Molecular biology

The human KCNQ2 and KCNQ3 cDNAs were kindly provided by Thomas J. Jentsch and all point mutants, deletion mutants and fusion proteins were created by PCR-based mutagenesis with LA taq (Takara). KCNQ2 and its mutants were tagged with three-tandem repeated FLAG epitopes (DYKDDDDK) at their N-terminus. All CD4 and CD4 mutant constructs were tagged with HA epitope (YPYDVPDYA). CD4-GFP60aa was generated by adding 60 C-terminal residues of green fluorescent protein to the C-terminus of CD4. CD4-ExtraC was constructed by appending ExtraC to the C-terminus of CD4. For whole-cell patch clamp recording, cycloheximide treatment, pulse-chase assay, surface biotinylation, ubiquitination assay and quantitative RT-PCR analysis, all cDNA clones used in these experiments were constructed and inserted into the pIRES2-EGFP vector (Clontech). For two-electrode voltage clamp recording, wild-type constructs of KCNQ2, KCNQ3, KCNQ5 and their mutants were introduced into the KSM vector (19). KCNQ2 and Q2-*2513del1bp* were constructed and inserted into pEGFPC2 (Clontech) for fluorescence microscopy.

Confocal fluorescence microscopy

For staining of localization in the ER, HEK293 cells were co-transfected with EGFP-KCNQ2 or EGFP-fsKCNQ2 (Q2-*2513del1bp*) and pDsRed2-ER (Clontech) using Lipofectamine 2000 (Invitrogen). After 36 h incubation,

cells were washed in phosphate buffered saline (PBS, containing 10 mM phosphate buffer, pH 7.4, 150 mM NaCl, 0.5 mM $MgCl_2$ and 1 mM $CaC1_2$) three times, and fixed in 4% paraformaldehyde/PBS for 15 min before washing in PBS three times. Slides were mounted with mounting medium and images were obtained using a confocal microscope (FV1000; Olympus). For staining of localization in the Golgi apparatus, cells transfected with EGFP-KCNQ2 or EGFP-fsKCNQ2 were fixed as above. Cells were permeabilized in 0.2% Triton X-100/PBS for 10 min, and blocked in 5% goat serum/PBS for 1 h prior to incubation for 2 h at room temperature with rat antibody against GM130 (a Golgi matrix protein) at dilution of 1:150 (BD Transduction Laboratories) with serum/PBS. Cells were washed in PBS three times, and then incubated for 1 h at room temperature with TRITC-conjugated anti-rat antibody (1:250; Zhongshanjinqiao, Beijing, China). After washing three times in PBS, slides were mounted with mounting medium and images were obtained using the same confocal microscope.

Electrophysiology

For whole-cell patch clamp recording, currents were recorded at room temperature using the EPC 10 UBS patch clamp amplifier (HEKA). Patch electrodes were pulled from borosilicate glass and had a final resistance of 3–5 MΩ, when filled with internal pipette solution which contained (in mM) 130 KCl, 3 NaCl, 1 $MgCl_2$, 5 EGTA, 10 HEPES, 5 glucose and 3 Mg-ATP at pH 7.3. Cells were perfused with the external solution containing (in mM) 140 NaCl, 4.7 KCl, 1.2 $MgCl_2$, 1 $CaCl_2$, 11 glucose and 5 HEPES at pH 7.4. Data were acquired and analyzed using PatchMaster software (HEKA).

For two-electrode voltage clamp recording, *Xenopus* oocytes (stages V and VI) were selected and injected with 46 nl of solution containing 10 ng of cRNA using a microinjector (Drummond Scientific Co.). 3 days after injection, oocytes were impaled with two microelectrodes (0.5–1.0 MΩ) filled with 3 M KCl in a 40 µl recording chamber, and whole cell currents were recorded using a two-electrode voltage clamp. The chamber was constantly perfused with ND-96 recording solution containing (in mM) 96 NaCl, 2 KCl, 1 $MgCl_2$, 1 $CaCl_2$, and 5 HEPES at pH 7.6. Currents were recorded in ND-96 solution at room temperature using a GeneClamp 500 amplifier (Axon Instruments) or an OC-725C amplifier (Warner Instruments). Data were acquired and analyzed using Pulse software (HEKA).

Cycloheximide treatment and Western blotting assay

For cycloheximide treatment, transfected Cos-7 cells were treated with cycloheximide for various time periods and then analyzed by Western blot. For Western blot assay, protein samples were loaded on SDS-PAGE and transferred onto nitrocellulose membranes (Millipore) before blocking with a blocking buffer of 5% powdered nonfat milk in TBS-T (Tris bufferred saline with 0.05% Tween 20). The membranes were incubated overnight at 4°C with primary antibody

(1:2000anti-HA from Roche; 1:4000, anti-FLAG from Sigma; 1:500 anti-actin and anti-GAPDH from Santa Cruz) diluted with blocking buffer. After washing with TBS-T three times, the membranes were incubated for 1 h at room temperature with their corresponding secondary HRP-coupled antibodies (1:5000 Santa Cruz) diluted with blocking buffer. After washing three times, signal was detected by using the Immobilon Western HRP substrate (Millipore).

Cell surface biotinylation assay

Confluent monolayers of HEK 293 cells transfected with FLAG-KCNQ2 or FLAG-fsKCNQ2 were washed three times with ice-cold Ca^{2+}/Mg^{2+} PBS. HEK293 cells were biotinylated with 0.5 mg/ml Sulfo-NHS-SS-biotin (Pierce) in Ca^{2+}/Mg^{2+} PBS, pH 7.4 for 30 min at 4°C. The remaining biotin was quenched by incubating the cells for an additional 10 min with 100 mM glycin in Tris buffered saline (TBS). The cells were then washed with PBS and incubated in RIPA lysis buffer containing 150 mM NaC1, 20 mM Tris, pH 8.0, 1% Nonidet P-40, 1% sodium deoxycholate, 0.1%SDS, 10 mM EDTA, and protease inhibitor cocktail (Roche) at 4 °C for 30 min. One fraction of cell lysate containing 200 µg protein was incubated with 20 µl of neutravidin beads (Pierce) for 2 h at 4°C, and the other fraction was prepared as total protein. After incubation, the beads carrying surface proteins were washed with RIPA lysis buffer and eluted with loading buffer. The total and surface proteins were both loaded onto 8% SDS-PAGE, and assayed by Western blotting.

Pulse-chase assay

HEK293 cells expressing HA-tagged CD4, or CD4-ExtraC were starved of methionine and cysteine for 1 h (with DMEM lacking methionine and cysteine), and then labeled with [35S]-methionine/cysteine (Easy Tag Express; Perkin Elmer) for 1 h. Cells were washed with PBS three times and incubated in regular DMEM for various time periods (0, 1, 2, 3 and 6 h). The cells were then washed twice in PBS and solubilized with RIPA lysis buffer. Cell lysate containing 200 µg of protein was incubated with Protein G-Sepharose (20 µl, GE Healthcare) and anti-HA antibody (1 µg, Roche) 4°C overnight. After washing three times with RIPA lysis buffer, the samples were dissolved in 30 µl of loading buffer, loaded onto 10% SDS-PAGE, and assayed by autoradiography.

Ubiquitination assay

Cos-7 cells transfected with a combination of cDNA constructs of FLAG-KCNQ2 or FLAG-fsKCNQ2 with HA-Ubiquitin (Ub) were harvested and lysed after expression for 24 h and treatment with MG132 for an additional 12 h. Cell lysate containing 200 µg of protein was incubated with Protein G-Sepharose (20 µl, GE Healthcare) and anti-FLAG antibody (1 µg, Sigma) 4°C overnight. Immunoprecipitates were washed three times in lysis buffer, dissolved in 30 µl of loading buffer and loaded onto 6% SDS-PAGE before immunoblotting with anti-HA (1:2000, Roche).

RNA extraction and quantitative RT-PCR amplification

Total RNA was extracted from HEK293

cells using the TRIZOL reagent (Invitrogen) according to manufacturer's protocol. A total of 10μg of RNA was treated with RNase-free Turbo DNase (Ambion) for 30 min at 37°C. RNA were extracted with phenol/chloroform, and precipitated with ethanol. The purified RNA was reverse-transcribed directly using the MMLV-RT, SPCL kit (Invitrogen) according to the manufacturer's protocol. After cDNA synthesis, real-time RT-PCR was performed with the 7500 Fast Real-Time PCR System (Applied Biosystems) using the SYBR Premix Ex Taq II kit (Takara) according to the manufacturer's protocol. Pairs of sequence specific primers used in this study are as follows: human KCNQ2, forward, 5'-GGCTTCAGCATCTCCCAGT-3'; reverse, 5'-GACTCTCCCTCCGCAATGTA-3'; and human GAPDH, forward, 5'-CCACTCCTCCACCTTTGAC-3'; reverse, 5'-ACCCTGTTGCTGTAGCCA-3'.

Statistics

All values are reported as mean ± s.e.m. Statistics were performed using Prism 4.0 software. Statistical significance was assessed using the *t*-test.

RESULTS

An extra segment derived from the distal C-terminal frame-shift mutation of KCNQ2 is responsible for current reduction.

The human mutant Q2-*2513del1bp* studied in this paper results from one nucleotide deletion at position 2513 bp, which was designated fsKCNQ2 (frame-shift mutant of KCNQ2). The fsKCNQ2 mutation results in a distal C-terminal deletion of the last seven amino acids before the stop codon which are replaced with an extra sequence of sixty-three amino acids (designated ExtraC). This fsKCNQ2 mutant does not change the intrinsic motifs or domains of the channel, as compared with wild type (WT) KCNQ2 (Figure 1). Another distal C-terminal frame-shift mutation in this study results from an insertion of five nucleotides at 2516 bp (designated Q2-*2516ins5bp*), leading to the generation of the same ExtraC (Figure 1). To investigate the mechanism by which these distal frame-shift mutations of KCNQ2 underlie BFNC, we began by confirming previous electrophysiological findings. Consistent with previous reports (13,14,16), expression of the fsKCNQ2 mutant in HEK293 cells or injection of its cRNA into oocytes resulted in small currents (Figure 2A & B).

To make sure the inhibitory effect of the fsKCNQ2 mutant on channel function was specifically mediated by the extended C-terminal segment (ExtraC), we generated a truncation mutant (Q2-838X) by deleting the extended C-terminus (63 amino acids) of the fsKCNQ2 mutant. In the Q2-838X mutant, the number with letter X stands for the amino acid mutated to the stop code where translation ends. The Q2-838X mutant without ExtraC expressed a robust current with gain-of-function (Figure 2B), suggesting that dysfunction of the fsKCNQ2 mutant is due to ExtraC causing current reduction.

KCNQ3 that functions as an auxiliary subunit has been shown to facilitate KCNQ2 function. To test

whether KCNQ3 can reverse the effect of this frame-shift mutation, we co-injected the cRNA of fsKCNQ2 with KCNQ3 into *Xenopus* oocytes. Co-injection of the fsKCNQ2 mutant with WT KCNQ3 failed to cause an increase in current expression, as compared with co-injection of WT KCNQ2 with KCNQ3, demonstrating that KCNQ3 can not rescue the function of the fsKCNQ2 mutant (Figure 2B). To confirm the effect of the ExtraC peptide, we appended it to the C-terminus of KCNQ5, another member of the KCNQ family. Consistent with the result of co-expression of fsKCNQ2 with KCNQ3, KCNQ5 with ExtraC appended (KCNQ5-ExtraC) resulted in significant reduction of current density when coexpressed with KCNQ3 (Figure 2C). These results show that the ExtraC derived from the C-terminal frame-shift mutations of KCNQ2 is responsible for current reduction.

Accelerated degradation of fsKSNQ2 by a ubiquitin-independent proteasome pathway

To examine whether the reduced current density of fsKCNQ2 mutant resulted from reduced surface expression, we used confocal fluorescence microscopy and biotin labeling for surface protein assay. We used the pDsRed2-ER plasmid to label the ER and the GM130 antibody (GM130) to stain the Golgi apparatus for identification of localization with wild type KCNQ2 or the fsKCNQ2 mutant by confocal imaging.

Similar to WT KCNQ2, fsKCNQ2 proteins were localized in both the ER and Golgi apparatus (Figure 3A), showing that the mutant can leave the ER and traffic to the Golgi apparatus. To relatively quantify surface expression, surface proteins WT KCNQ2 or fsKCNQ2 expressed in HEK293 were labeled by biotin and analyzed by Western blotting. Biotin labeling showed that both surface and total protein of the fsKCNQ2 mutant were much less than WT KCNQ2 (Figure 3B). These results suggest that decreased surface fsKCNQ2 which underlies the reduced current density is likely due to the reduction of the total amount of fsKCNQ2 protein (Figure 3B). To eliminate the possibility of protein reduction caused by reduced plasmid transfection or gene transcription of fsKCNQ2, we also quantified KCNQ2 mRNA by quantitative RT-PCR. Cells tranfected with WT KCNQ2 or fsKCNQ2 plasmid showed little difference in mRNA quantity (Figure 3C), demonstrating that neither transfection nor transcription were affected. These results suggest that reduced surface expression of the mutant protein likely results from increased protein degradation.

To test the stability of fsKCNQ2, we treated Cos-7 cells expressing fsKCNQ2 with the protein synthesis blocker cycloheximide (CHX) and evaluated protein stability by Western blotting of remaining proteins after degradation. After 12 h of CHX treatment, the half-life of fsKCNQ2 was about 4 h. In contrast, the half-life of WT KCNQ2 was over 12 h (Figure 4A). This result of this shortened half-life of these mutant proteins was also confirmed in both HEK293 and CHO cells (Supplemental Figure 1). These results indicate that fsKCNQ2 protein degradation is accelerated, leading to reduced surface

expression.

Proteasome and lysosome pathways are widely considered to be mechanisms for protein degradation. Using the proteasome-specific inhibitor MG132 or the lysosome-specific inhibitor chloroquine, we sought to determine whether fsKCNQ2 protein degradation is mediated by these two pathways. In WT KCNQ2 expressing Cos-7 cells treated with CHX, KCNQ2 protein showed no obvious difference in degradation in the presence or absence of either chloroquine or MG132 (Figure 4B, top panels). In contrast, Cos-7 cells expressing the fsKCNQ2 mutant that were treated only with CHX resulted in significant protein degradation that was inhibited upon treatment with MG132, as compared with the chloroquine group (Figure 4B, bottom panels). These results show that the proteasome pathway, and not the lysosome pathway, underlies the destabilization of fsKCNQ2 mutant protein.

We next investigated whether accelerated proteasome-dependent degradation of fsKCNQ2 is due to ubiquitination of this mutant. To test for ubiquitination of the fsKCNQ2 mutant, Cos-7 cells expressing different combinations of HA-Ub, FLAG-KCNQ2 and FLAG–fsKCNQ2 were treated with MG132 for 12 h. Proteins were subject to immunoprecipitation with anti-FLAG antibody, and Western blotted with anti-HA antibody. Ubiquitination of a target protein resulted in smeared bands at high molecular weight (Figure 4C). As a control, WT KCNQ2 was subjected to ubiquitination, as previously demonstrated in a similar assay (20). Similar to WT KCNQ2, the fsKCNQ2 mutant showed no further ubiquitination when it was co-expressed with HA-Ub proteins (Figure 4C). This result indicates that the proteasome-dependent degradation of fsKCNQ2 does not rely on ubiquitination.

The ExtraC peptide serves as a degradation signal that is transferable

To test whether the degradation effect of the ExtraC peptide can be transferred to another unrelated protein, we fused the ExtraC to the C-terminus of CD4 (CD4-ExtraC). As a control, we attached the C-terminus of CD4 to GFP60aa (C-terminal 60 residues of green fluorescent protein). GFP60aa contains the same number of residues as ExtraC. After CHX treatment for 7 h in HEK293 cells, CD4-ExtraC was dramatically degraded with a half-life of about 1.5 h, as compared with WT CD4 or CD4-GFPC60aa that had a half-life of more than 6 h, showing that the function of ExtraC which is specific for protein degradation is transferable (Figure 5A).

To further confirm this result, we used the metabolism inhibitor-free pulse-chase assay in which newly synthesized proteins were labeled by S^{32}, and then evaluated for isotope labeled CD4 and CD4-ExtraC proteins over a period of 6 h. Appending the ExtraC to the C-terminus of CD4 resulted in fast degradation (Figure 5B), further demonstrating the transferability of ExtraC which was identified as a degradation signal.

Identification of key motif/residues within ExtraC critical for degradation

To identify the key motif/residues within ExtraC which mediate degradation, we constructed several deletions of fsKCNQ2. Serial C-terminal deletions of fsKCNQ2 were designated as fsQ2-869X, -865X, -860X, -853X, and -845X, in which the three digit numbers represent the position of the amino acid mutated to the stop codon that is designated as X. Whole-cell patch clamp recordings of HEK293 cells expressing either fsKCNQ2 or truncated mutants fsQ2-869X and fsQ2-865X resulted in significant reduction of current density, as compared with the robust current expression of WT KCNQ2 or truncated mutants fsQ2-860X, fsQ2-853X and fsQ2-845X (Figure 6A left panel). Comparison of fsQ2-860X and fsQ2-865X reveals the motif RCLRG containing five residues which distinguishes the two mutants (Figure 6A). fsKCNQ2 and two truncated mutants that all carry this RCLRG motif showed a small amount of current, which was in contrast with WT KCNQ2 and mutants without the motif that showed robust current expression (Figure 6A left panel). To investigate whether reduced currents were due to degradation, we transfected WT KCNQ2 and the three mutants fsQ2-865X, fsQ2-860X and fsKCNQ2 into Cos-7 cells treated with or without CHX (75 μg/ml) for 12 h. Blocking protein synthesis with CHX revealed that both fsQ2-865X truncation and fsKCNQ2 mutant proteins showed fast degradation, as compared with either fsQ2-860X or WT KCNQ2 (Figure 6A right panel).

Degradation signals can transfer their function when they are attached to either the N- or C- protein terminus (17,21,22). To test whether the function of ExtraC can be transferred to the N-terminus, we attached ExtraC to the N-terminus of WT KCNQ2 (ExtraC-KCNQ2) and made several N-terminal truncation mutants based on ExtraC-KCNQ2 designated as ExtraC-del15-Q2, ExtraC-del22-Q2, ExtraC-del27-Q2, ExtraC-del31-Q2 and ExtraC-del41-Q2 (Figure 6B left panel). Whole-cell recordings of HEK293 cells expressing ExtraC-KCNQ2 or the two N-terminal deletion mutants, ExtraC-del15-Q2 and ExtraC-del22-Q2 showed dramatic reduction of current, as compared with robust current expression associated with either WT KCNQ2 or its counterparts ExtraC-del27, -del31 and -del41-Q2, in which the RCLRG motif was removed (Figure 6B left panel). To further test the effect of the RCLRG motif on protein degradation, we transfected WT KCNQ2 and three mutants ExtraC-KCNQ2, ExtraC-del22-Q2 and ExtraC-del27-Q2 into Cos-7 cells. Consistent with current recordings, protein degradation of either ExtraC-del22-Q2 or ExtraC-KCNQ2 was faster than that of WT KCNQ2 or ExtraC-del27-Q2 without the RCLRG motif (Figure 6B right panel). These results demonstrate that the degradation function of ExtraC with the RCLRG motif can be conferred upon both N- and C-termini of channel proteins.

To further identify which individual residues are critical in mediating degradation, we mutated each of the five residues within the RCLRG motif into alanine. As shown in Figure 7, the fsQ2-865X (fsQ2-860-RCLRG) mutant showed rapid degradation (middle

panels), as compared with WT KCNQ2 (left panels). Mutating the first two individual residues of the RCLRG motif to alanine in either the N- or C-terminus abolished accelerated degradation. In contrast, the fsQ2-860-RCARG mutant in which the middle residue leucine was mutated had no affect on degradation (Figure 7, middle panels). To further confirm the two flanking residues of the RCLRG motif were critical for degradation, we generated two double mutations. As shown in Figure 7 (right panels), the two double mutations prevented degradation, further confirming the two flanking residues necessary for degradation (Figure 7, right panels). These results indicate that the four residues of the RCXRG motif play a critical role in mediating accelerated degradation effect of the ExtraC in fsKCNQ2 mutant (Figure 7).

DISCUSSION

Most human BFNC mutations which have been identified are located in the C-terminus of the Kv7.2/KCNQ2 channel. However, none of the mutations that have been tested show their dominant-negative effects on wild-type subunits (5,6,11,12). This indicates that BFNC is caused by haploinsufficiency, suggesting the Kv7.2/KCNQ2 mutant protein produced by the cell is not sufficient to function normally.

To better understand the mechanism by which channel mutations which show partial dominant-negative effects underlie epilepsy, we studied the two distal C-terminal frame-shift mutations of KCNQ2 that exhibit normal biophysical properties of channel function, but have reduced current density (13,14,16). Based on their functional properties, we reasoned that the frame-shift KCNQ2 mutations can fold properly and be transported to the plasma membrane. To verify this concept we carried out staining of one of the mutations tagged with GFP in HEK293 cells, and the results show that those C-terminal mutations can be translocated across from ER to the Golgi and plasma membrane and distributed in the same fashion as WT KCNQ2 (Figure 3A & B). This is consistent with previous reports which have noted that there is little difference in the distribution in the axon and the axon initial segment (AIS) in neurons and translocation across Golgi and plasma membranes (15,16), suggesting that the fsKCNQ2 mutant channel is correctly folded. In contrast, the frame-shift mutation Q2-*2043del1bp* with a much larger frame-shift region (219 amino acids), can not form functional channels and cannot be transported from the ER to the Golgi. This mutant is thought to be degraded through the ER associated degradation (ERAD) pathway which degrades misfolded proteins (16,23,24). Based on the findings of this study, we propose a novel degradation mechanism which removes frame-shift mutant proteins with normal folding that carry a degradation signal.

Is the degradation signal within the extended C-terminus specific for channel degradation? To address this question, we constructed another frame-shift mutant Q2-*2513del2bp* in which two nucleotides are deleted, as compared with the fsKCNQ2 mutant (Q2-*2513del1bp*) where only one

nucleotide is deleted. This Q2-*2513del2bp* mutation introduces another extra C-terminal sequence with 39 amino acids that does not contain the RCXRG motif. However, this frame-shift mutant reveals no difference in degradation, as compared with WT KCNQ2 (Supplemental Figure 2), indicating that random frame-shift mutations without the RCXRG motif have no effect on protein stability. Regarding the role of the RCXRG motif within ExtraC as a general signal for degradation (Figure 5 & Figure 6B), we propose that any mutant protein with the RCXRG motif within a degradation signal will be subject to accelerated breakdown.

Why is it so easy to create a degradation signal in such a short extra region? Do native proteins with longer sequences contain degradation signals? Correctly folded proteins may carry numerous degradation signals. However, these signals are likely sequestered or enfolded in structured proteins or assembled with auxiliary subunits, in which case they may not be functional (17). When correct folding goes awry due to truncation or mutation at key sites, these signals may become exposed and functional (17,25,26). Based on our findings, we suspect that these distal frame-shift mutations may have minor changes of their original sequence as most parts of mutant proteins can be folded correctly in the manner of wild type proteins. When mutations cause random rearrangement of codons after site mutation, random sequences that are not properly structured as native proteins selected by evolution can be created (27-29), thus generating signals that are exposed resulting in protein degradation. Without specific structural information, we speculate that the ExtraC polypeptide of the fsKCNQ2 mutant may be highly disordered or unstructured due to its random codon rearrangement (27-29). This property of ExtraC may facilitate RCXRG motif recognition by degradation-related molecules (30,31). On the other hand, the disordered ExtraC may provide necessary unstructured initials for proteasome digestion (32,33).

Does the degradation signal from the ExtraC have any implications for actual physiological degradation since the signal is generated from a random mutagenesis? We performed literature and database search to look into whether the RCXRG motif exists as a physiological degradation signal in native proteins. We have found that many native proteins contain the RCXRG motif, but there is no report that native proteins carrying the RCXRG motif are subject to physiological degradation. This suggests that the RCXRG motif/ExtraC may not have any physiological implications. However, the motif/degradation signal can be hidden or become non-functional when native proteins with degradation signal have structures (17). When unstructured in an environment such as oxidative stress, native proteins can be subject to degradation (34,35). It has also been shown that a random distal C-terminal frame-shift mutation of aquaporin-2 (water channel protein) can result in generating an extra region that contains several signal motifs for

basolateral sorting or retention (36). Those signal motifs from aquaporin-2 mutation have been demonstrated in other native proteins (for instance, Low Density Lipoprotein receptors), functioning as physiological signals for basolateral sorting and retention (37-40).

In summary, we have identified a novel degradation signal that is derived from distal C-terminal frame-shift mutations of KCNQ2, which causes the impairment of channel function leading to epilepsy. This degradation signal contains a primary critical motif of five-amino acids (RCXRG) that can be transferred to non-channel proteins for degradation. Our findings demonstrate that the distal C-terminal frame-shift mutations of the Kv7.2/KCNQ2/M-channel are subject to degradation through the ubiquitin-independent proteasome pathway, a cellular mechanism by which incomplete dominant-negative mutations of Kv7.2/KCNQ2 cause epilepsy of infancy. Here, we propose a novel degradation mechanism which removes mutant proteins that carry the degradation signal, serving as a general mechanism for clearance of numerous mutant proteins in the cell. Moreover, identification and removal of this degradation signal may potentially help production of functional recombinant proteins that are of importance for pharmaceutical manufacture.

REFERENCES

1. Jentsch, T. J., Schroeder, B. C., Kubisch, C., Friedrich, T., and Stein, V. (2000) *Epilepsia* **41**, 1068-1069
2. Psenka, T. M., and Holden, K. R. (1996) *Seizure* **5**, 243-245
3. Ronen, G. M., Rosales, T. O., Connolly, M., Anderson, V. E., and Leppert, M. (1993) *Neurology* **43**, 1355-1360
4. Charlier, C., Singh, N. A., Ryan, S. G., Lewis, T. B., Reus, B. E., Leach, R. J., and Leppert, M. (1998) *Nature Genetics* **18**, 53-55
5. Biervert, C., Schroeder, B. C., Kubisch, C., Berkovic, S. F., Propping, P., Jentsch, T. J., and Steinlein, O. K. (1998) *Science* **279**, 403-406
6. Schroeder, B. C., Kubisch, C., Stein, V., and Jentsch, T. J. (1998) *Nature* **396**, 687-690
7. Wang, H. S., Pan, Z., Shi, W., Brown, B. S., Wymore, R. S., Cohen, I. S., Dixon, J. E., and McKinnon, D. (1998) *Science* **282**, 1890-1893
8. Watanabe, H., Nagata, E., Kosakai, A., Nakamura, M., Yokoyama, M., Tanaka, K., and Sasai, H. (2000) *J Neurochem* **75**, 28-33
9. Peters, H. C., Hu, H., Pongs, O., Storm, J. F., and Isbrandt, D. (2005) *Nat Neurosci* **8**, 51-60
10. Volkers, L., Rook, M. B., Das, J. H. G., Verbeek, N. E., Groenewegen, W. A., van Kempen, M. J. A., Lindhout, D., and Koeleman, B. P. C. (2009) *Neuroscience Letters* **462**, 24-29
11. Richards, M. C., Heron, S. E., Spendlove, H. E., Scheffer, I. E., Grinton, B., Berkovic, S. F., Mulley, J. C., and Davy, A. (2004) *Journal of Medical Genetics* **41**, -
12. Peroz, D., Rodriguez, N., Choveau, F., Baro, I., Merot, J., and Loussouarn, G. (2008) *Journal of Physiology-London* **586**, 1785-1789
13. Singh, N. A., Westenskow, P., Charlier, C., Pappas, C., Leslie, J., Dillon, J., Anderson, V. E., Sanguinetti, M. C., and Leppert, M. F. (2003) *Brain* **126**, 2726-2737
14. Lerche, H., Biervert, C., Alekov, A. K., Schleithoff, L., Lindner, M., Klingler, W., Bretschneider, F., Mitrovic, N., Jurkat-Rott, K., Bode, H., Lehmann-Horn, F., and Steinlein, O. K. (1999) *Annals of Neurology* **46**, 305-312
15. Chung, H. J., Jan, Y. N., and Jan, L. Y. (2006) *Proceedings of the National Academy of Sciences of the United States of America* **103**, 8870-8875
16. Soldovieri, M. V., Castaldo, P., Iodice, L., Miceli, F., Barrese, V., Bellini, G., del Giudice, E. M., Pascotto, A., Bonatti, S., Annunziato, L., and Taglialatela, M. (2006) *Journal of Biological Chemistry* **281**, 418-428
17. Ravid, T., and Hochstrasser, M. (2008) *Nature Reviews Molecular Cell Biology* **9**, 679-U625
18. Schrader, E. K., Harstad, K. G., and Matouschek, A. (2009) *Nature Chemical Biology* **5**, 815-822
19. Jow, F., and Wang, K. (2000) *Brain Res Mol Brain Res* **80**, 269-278
20. Ekberg, J., Schuetz, F., Boase, N. A., Conroy, S. J., Manning, J., Kumar, S., Poronnik, P., and Adams, D. J. (2007) *J Biol Chem* **282**, 12135-12142
21. Tasaki, T., and Kwon, Y. T. (2007) *Trends in Biochemical Sciences* **32**, 520-528
22. Li, X. Q., and Coffino, P. (1993) *Molecular and Cellular Biology* **13**, 2377-2383
23. Meusser, B., Hirsch, C., Jarosch, E., and Sommer, T. (2005) *Nature Cell Biology* **7**, 766-772
24. Brodsky, J. L., and Vembar, S. S. (2008) *Nature Reviews Molecular Cell Biology* **9**, 944-U930
25. Chen, H., MacDonald, A., and Coffino, P. (2002) *Journal of Biological Chemistry* **277**,

45957-45961
26. Vembar, S. S., and Brodsky, J. L. (2008) *Nature Reviews Molecular Cell Biology* **9**, 944-U930
27. Yamauchi, A., Yomo, T., Tanaka, F., Prijambada, I. D., Ohhashi, S., Yamamoto, K., Shima, Y., Ogasahara, K., Yutani, K., Kataoka, M., and Urabe, I. (1998) *Febs Letters* **421**, 147-151
28. Doi, N., and Yanagawa, H. (1998) *Cellular and Molecular Life Sciences* **54**, 394-404
29. Doi, N., Kakukawa, K., Oishi, Y., and Yanagawa, H. (2005) *Protein Engineering Design & Selection* **18**, 279-284
30. Fuxreiter, M., Tompa, P., and Simon, I. (2007) *Bioinformatics* **23**, 950-956
31. Dyson, H. J., and Wright, P. E. (2005) *Nature Reviews Molecular Cell Biology* **6**, 197-208
32. Prakash, S., Tian, L., Ratliff, K. S., Lehotzky, R. E., and Matouschek, A. (2004) *Nature Structural & Molecular Biology* **11**, 830-837
33. Komaru, K., Ishida, Y., Amaya, Y., Goseki-Sone, M., Orimo, H., and Oda, K. (2005) *Febs Journal* **272**, 1704-1717
34. Ferrington, D. A., Sun, H., Murray, K. K., Costa, J., Williams, T. D., Bigelow, D. J., and Squier, T. C. (2001) *J Biol Chem* **276**, 937-943
35. Kurepa, J., and Smalle, J. A. (2008) *Plant Signal Behav* **3**, 386-388
36. Kamsteeg, E. J., Bichet, D. G., Konings, I. B. M., Nivet, H., Lonergan, M., Arthus, M. F., van Os, C. H., and Deen, P. M. T. (2003) *Journal of Cell Biology* **163**, 1099-1109
37. Ohno, H., Fournier, M. C., Poy, G., and Bonifacino, J. S. (1996) *J Biol Chem* **271**, 29009-29015
38. Sorkin, A., Nesterov, A., Carter, R. E., Sorkina, T., and Gill, G. N. (1999) *Embo Journal* **18**, 2489-2499
39. Hunziker, W., Harter, C., Matter, K., and Mellman, I. (1991) *Cell* **66**, 907-920
40. Folsch, H., Ohno, H., Bonifacino, J. S., and Mellman, I. (1999) *Cell* **99**, 189-198

Acknowledgements:
We would like to thank our laboratory members Ms. Yanxin Lu, Dr. Ping Liang, Mr. Ka Lu and Ms. Wen Liu for their assistance and comments on this work. We would also like the thank Dr. Michael A McNutt for evaluation and correction of English in this manuscript. KWW wishes to thank J. M. Wang for her consistent support during this research.

FOOTNOTES

This work was supported by research grants to KWW from the National Science Foundation of China, 30630017 and 30970919; and from the Ministry of Science Technology of China, '973 Program' 2007CB512100, and from the Ministry of Education of China, 111 Project China (B07001).

To whom correspondence may be addressed: Peking University School of Medicine, 38 Xueyuan Road, Beijing 100091; wangkw@bjmu.edu.cn or wangkw@hsc.pku.edu.cn; Tel: (8610) 82805065; Fax: (8610) 82805065

The abbreviations used are: bp, base pair; CHX, cycloheximide; GFP, green fluorescent protein; Ub, ubiquitin; CQ, chloroquine

FIGURE LEGENDS

FIGURE 1. Schematic presentation of wild type KCNQ2 and the distal C-terminal frame-shift mutations in KCNQ2. The Kv7.2/KCNQ2 channel has six transmembrane domains and a long C-terminus which contains important functional motifs and domains. The two distal frame-shift mutants, Q2-*2513del1bp* and Q2-*2516ins5bp* result from a one nucleotide deletion at 2513 bp, and *a* 5-nucleotide insertion at bp in the human KCNQ2 gene, respectively. As a result, the fsKCNQ2 mutant (Q2-*2513del1bp)* is truncated and lacks seven terminal amino acids; and the Q2-*2516ins5bp* mutant is truncated and lacks the last five amino acids Both mutations are replaced with a peptide of 63 amino acids at their C-terminus (designated ExtraC in this study), as compared with wild-type (WT) human KCNQ2 (KCNQ2) with 844 residues. The C-terminal amino acids are represented as a one-letter symbol in the protein sequence. The italicized characters and numbers represent the mutation of the nucleotide sequence; non-italicized numbers indicate the residue in the protein sequence. IQ: calmodulin binding motif; A domain: channel assembly domain; AnkG: Ankyrin-G binding motif.

FIGURE 2. Current reduction in KCNQ channel mutations containing the ExtraC peptide. (A) Current traces were recorded by whole-cell patch clamp in HEK293 cells expressing KCNQ2 (left panel) or fsKCNQ2 (middle panel). Cells were held at -80 mV in response to a family of depolarizing potentials from -80 mV to +40 mV with 10-mV increments for 1 second. The rightmost panel shows their peak current density determined at the end of 1 second depolarization of +40 mV. Data are expressed as mean ± s.e.m. (n=5-7, ***, p <0.001). (B) Representative current traces were recorded from *Xenopus laevis* oocytes by a two-electrode voltage clamp. The upper panels show comparison of current amplitudes of KCNQ2, fsKCNQ2 and KCNQ2-838X. The bottom panels show comparison of co-expression of KCNQ2 or fsKCNQ2 with KCNQ3. Oocytes from the same batch of cells were injected with identical amounts of cRNA were held at -80 mV in response to a family of depolarizing potentials from -80 mV to +40 mV in 10 mV increments for 2.5 seconds. The rightmost upper and bottom panels summarize the peak current amplitudes determined at the end of 2.5-second depolarization of +40 mV. Data are expressed as mean ± s.e.m. (n=5-7, ***, p <0.001). (C) Representative current traces were recorded with a two-electrode voltage clamp from *Xenopus laevis* oocytes expressing KCNQ5 and KCNQ3, or KCNQ5-ExtraC (the ExtraC peptide was appended to the C-terminus of KCNQ5) and KCNQ3 using the same pulse protocol as in (B). The rightmost panel summarizes the peak current amplitudes determined at the end of 2.5-second depolarization of +40 mV. Data are expressed as mean ± s.e.m. (n=4-7, ***, p <0.001).

FIGURE 3. Reduced surface expression of fsKCNQ2 is a result of total protein reduction, and is not due to ER retention. (A) Left panels, confocal imaging of HEK293 cells co-transfected with plasmids of either EGFP-KCNQ2, or EGFP-fsKCNQ2

(green) and pDsRed2-ER for ER staining (red) after fixation with paraformaldehyde. Right panels, confocal imaging of HEK293 cells transfected with plasmids of either EGFP-KCNQ2, or EGFP-fsKCNQ2 (green) for Golgi staining with GM130 antibody (red). Bar indicates 20 μm. (B) Western blotting analysis of biotin-labeled surface KCNQ2 and fsKCNQ2 proteins. The surface proteins from HEK293 cells transfected with FLAG-KCNQ2 or FLAG-fsKCNQ2 plasmids were labeled by biotin and segregated by avidin beads. Surface protein and total protein were separated by SDS-PAGE and Western blotted with anti-FLAG or anti-actin antibody. In the lower panels, surface FLAG-tagged KCNQ2 and fsKCNQ2 proteins over actin or total FLAG-tagged KCNQ2 and fsKCNQ2 proteins over actin were normalized to that of KCNQ2 over actin. Data are expressed as mean ± s.e.m. (n = 3, ***, p <0.001). (C), Quantitative analysis of mRNA for KCNQ2 and fsKCNQ2 expressed in HEK293 cells lysed with Trizol reagent. Total RNA was extracted from the lysate, treated with DNase and quantified by quantitative RT-PCR analysis. There is no obvious difference in the quantity of mRNA in KCNQ2 and fsKCNQ2. Data are expressed as mean ± s.e.m. (n=3, n.s., p>0.05).

FIGURE 4. Accelerated degradation of fsKCNQ2 mediated by the ubiquitin-independent proteasome pathway. (A) CHX treatment assay of KCNQ2 and fsKCNQ2 in Cos-7 cells. Cells were transfected with plasmids FLAG-KCNQ2 or FLAG-fsKCNQ2 and treated with protein synthesis inhibitor CHX (Cycloheximide, 75 μg/ml) for the indicated time period (0, 4, 8 or 12 hours). After degradation, the remaining proteins were separated by SDS-PAGE, and analyzed by Western blotting using anti-FLAG or anti-actin antibody. Data are expressed as mean ± s.e.m. (n=4, *, p <0.05, **, p <0.01). The half-life of KCNQ2 is more than 12 h, and the half life of fsKCNQ2 is about 4 h. (B) Western blotting analysis of KCNQ2 and fsKCNQ2 in Cos-7 cells treated with CHX (75 μg/ml) and chloroquine (CQ, 50 μM) or MG132 (15 μg/ml). Samples were loaded in lanes from the left in the following order: control without any treatment, DMSO treatment for 8 h, CHX for 8 h, CHX with chloroquine for 8 h, CHX with MG132 for 8 h. Data were normalized to that of control without any treatment, and are expressed as mean ± s.e.m. (n=3, **, p <0.01, n.s., p >0.05) (C) Cos-7 cells were transfected with combinations of FLAG-KCNQ2 or FLAG-fsKCNQ2 and HA-Ubiquitin plasmids as indicated with a plus sign, and treated with MG132 for 12 h. Cell lysates were subjected to immunoprecipitation (IP) by anti-FLAG antibody before Western blotting with anti-HA antibody. As a loading control, lysates were directly Western blotted with anti-HA or anti-FLAG antibody.

FIGURE 5. The degradation function of ExtraC is transferable to CD4 protein. (A) HEK293 cells transfected with HA-tagged plasmids of CD4 (left panels, as a blank control), CD4-GFP60aa (middle left panels, as a negative control), or CD4-ExtraC (middle right panels) were treated with CHX for the indicated time period (0, 1, 3 or 7 h). Proteins were separated by SDS-PAGE, and Western blotted with anti-HA or anti-GAPDH antibody. CD4-GFP60aa is a chimera of CD4 with 60 residues from the C-terminal sequence of GFP appended, and the number of residues is approximately

the same as ExtraC. The rightmost plot shows a summary of protein degradation over time. Both the half-lifes of CD4 and CD4-GFP60aa are more than 6 h, and that of CD4-ExtraC is about 1.5 h. (B) Pulse-chase analysis of protein degradation for CD4 (left panel) and CD4-ExtraC proteins (middle panel). Cells transfected with CD4 or CD4-ExtraC plasmids were labeled with S^{35} Met/Cys culture medium for 1 h followed by a chase with 'cold' Met/Cys culture medium for indicated time periods (0, 1, 2, 3 or 6 h). The same amount product from chase incubations were immunoprecipated using anti-HA antibody, and separated by SDS-PAGE for analysis by autoradiography. In the rightmost panel, the plot summarizes the protein degradation over time, and it is fitted with linear regression.

FIGURE 6. Functional identification of the RCLRG motif critical for current reduction and accelerated degradation. (A) Left panels: current densities of HEK293 cells expressing KCNQ2, fsKCNQ2, or fsKCNQ2 truncation mutants: fsQ2-845X, -853X, -860X, -865X and -869X (the number indicates amino acid sequence number of fsKCNQ2 that was mutated to a stop codon). Currents were recorded by whole-cell patch clamp in cells held at -80 mV and depolarized to +40 mV for 1 second. Data are expressed as mean ± s.e.m. (n=4-7). In the right panels, Western blotting analysis of proteins from transfected Cos-7 cells treated with CHX (75 μg/ml) for 0 or 12 h, or with vehicle (0.75‰ DMSO) for 12 h. Proteins were extracted, separated by SDS-PAGE and Western blotted with anti-FLAG or anti-actin antibody. (B) Left panels, current densities of HEK293 cells expressing KCNQ2 or ExtraC-KCNQ2 chimeras in which the ExtraC peptide and its truncations were fused to the N-terminus of KCNQ2. ExtraC truncations were generated from N-terminal deletions of the ExtraC-KCNQ2 chimera, leading to ExtraC-del15-Q2, ExtraC-del22-Q2, ExtraC-del27-Q2, ExtraC-del31-Q2 and ExtraC-del41-Q2 mutants. Currents were recorded by whole-cell patch clamp in cells held at -80 mV and depolarized to +40 mV for 1 second. Data are expressed as mean ± s.e.m. (n=4-6). Right panels: Western blotting analysis of proteins from transfected Cos-7 cells treated with CHX (75 μg/ml) for 0 or 12 h, or vehicle for 12 h as above in A.

FIGURE 7. Identification of residues within the RCLRG motif critical for protein degradation by alanine scanning mutagenesis. Cos-7 cells expressing wild-type KCNQ2, fsQ2-865X or different forms of the fsQ2-865X mutant in which each residue of the RCLRG motif was mutated to alanine (-ACLRG, -RALRG, –RCARG, –RCLAG, -RCLRA) or two residues were mutated to alanine (-AALRG and –RCLAA). The fsQ2-865X mutant has 864 residues (see Figure 1) and carries the RCLRG motif before the stop codon as indicated by the letter X. Cells were treated with CHX (75 μg/ml) for 0 or 12 h, or with vehicle (0.75‰ DMSO) for 12 h. All extracted proteins (left panels for KCNQ2, middle panels for fsQ2-865X and individual mutations, and right panels for double mutations of the fsQ2-865X mutant) were separated by SDS-PAGE and Western blotted with anti-FLAG or anti-actin antibody.

Figure 1

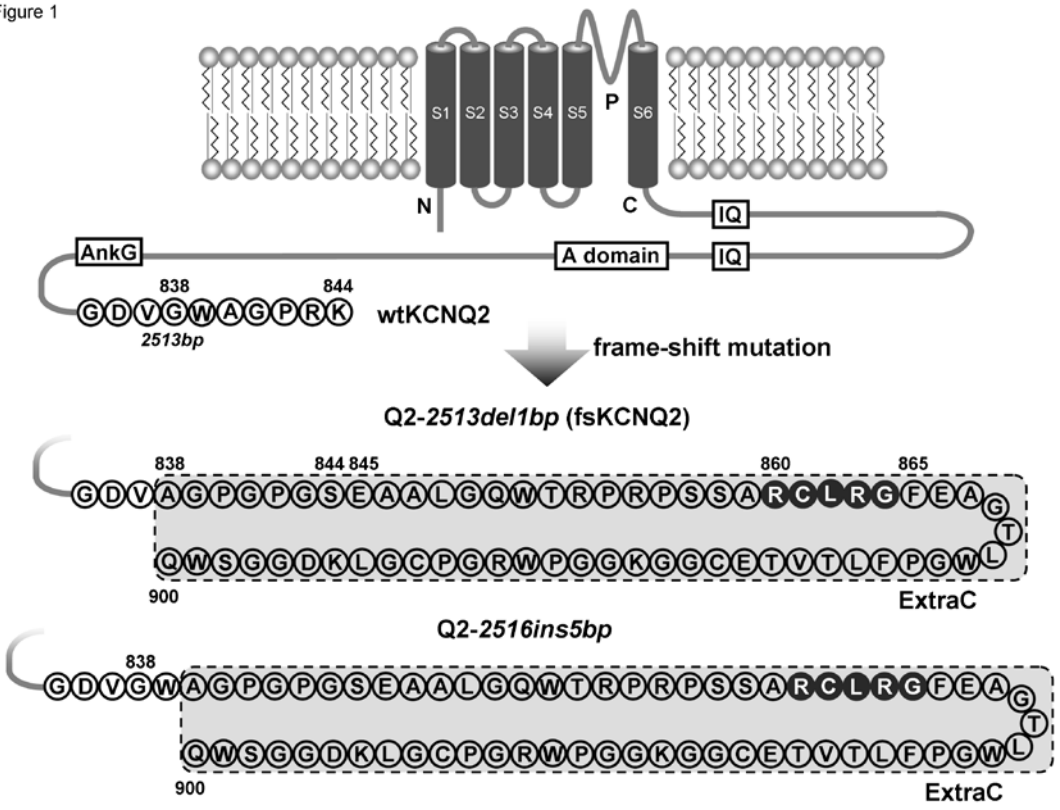

Figure 2

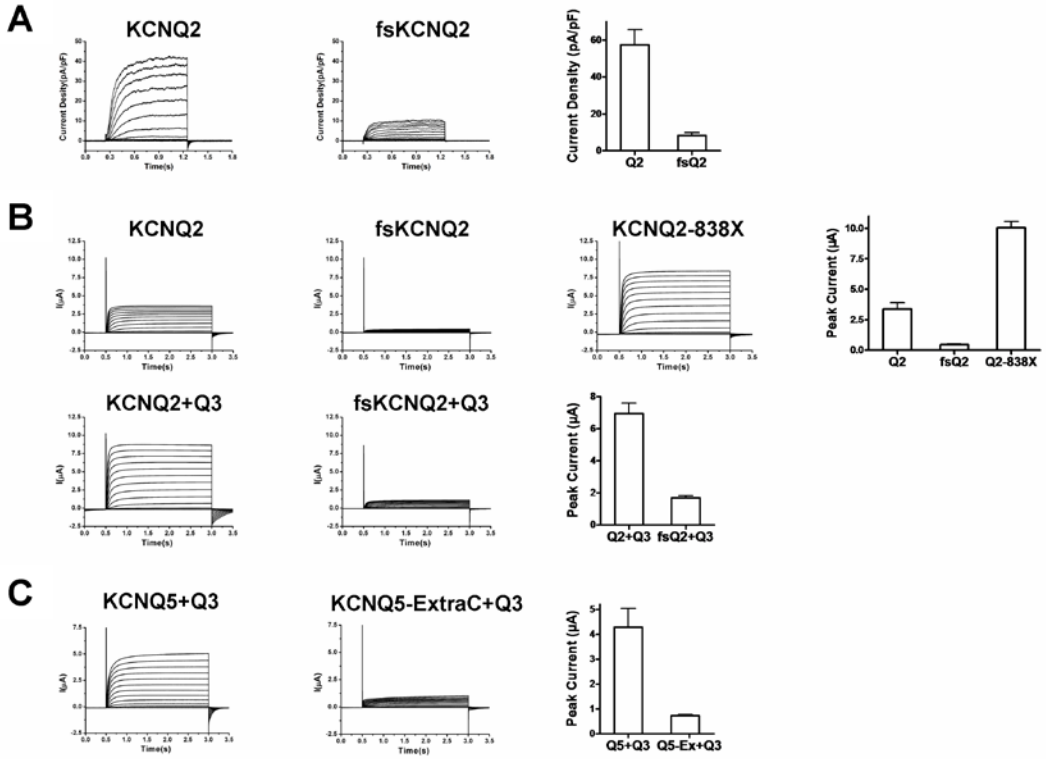

Figure 3

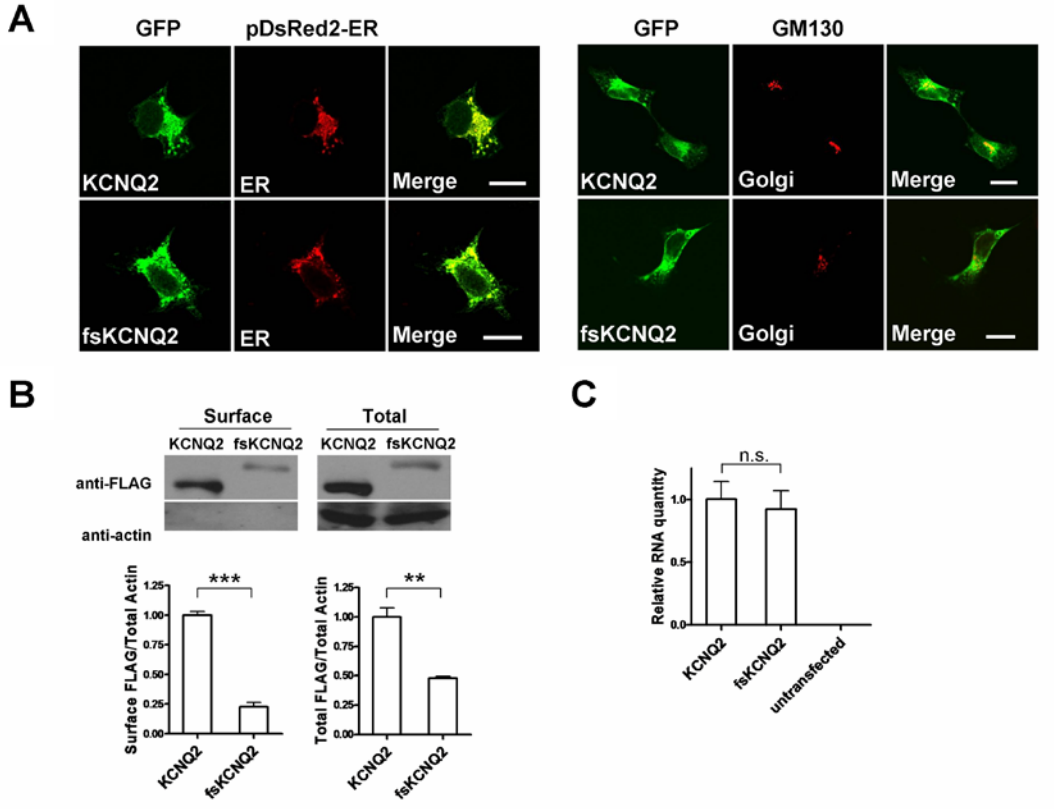

Figure 4

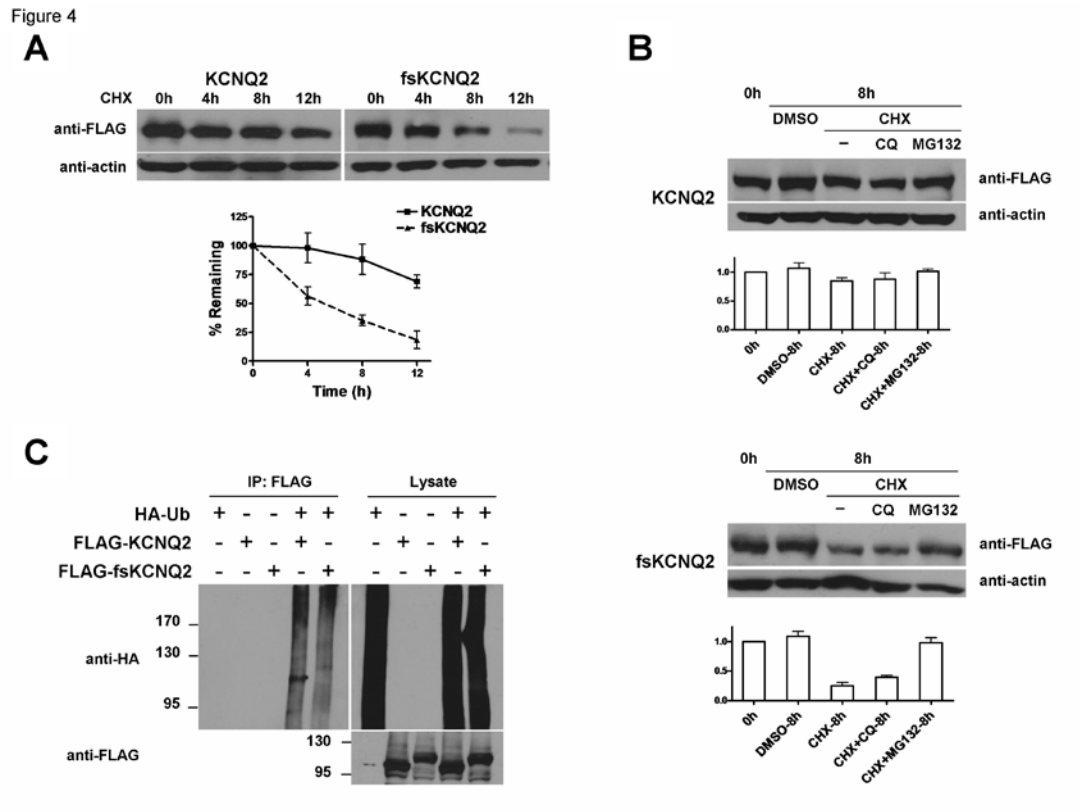

Figure 5

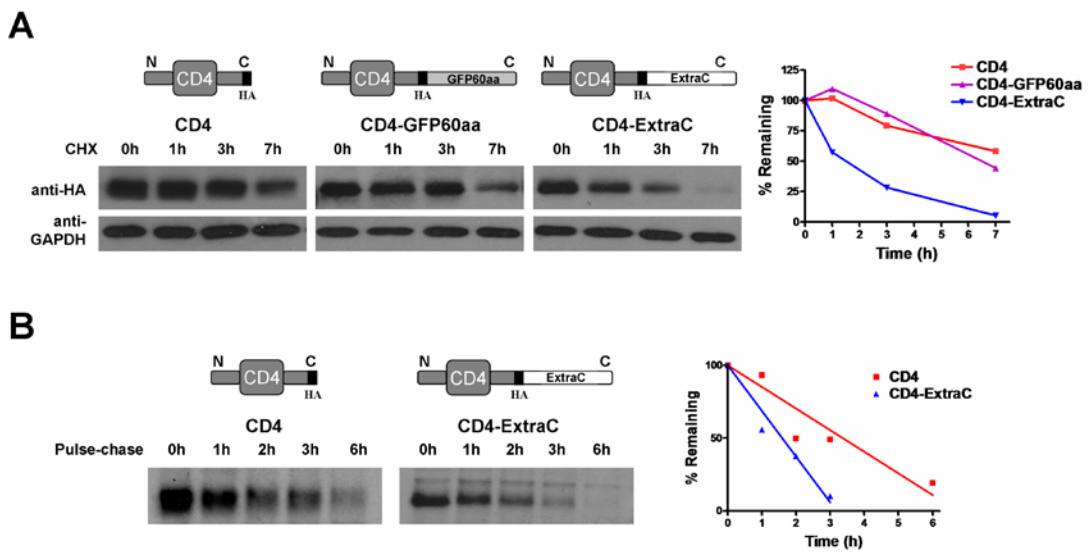

Figure 6

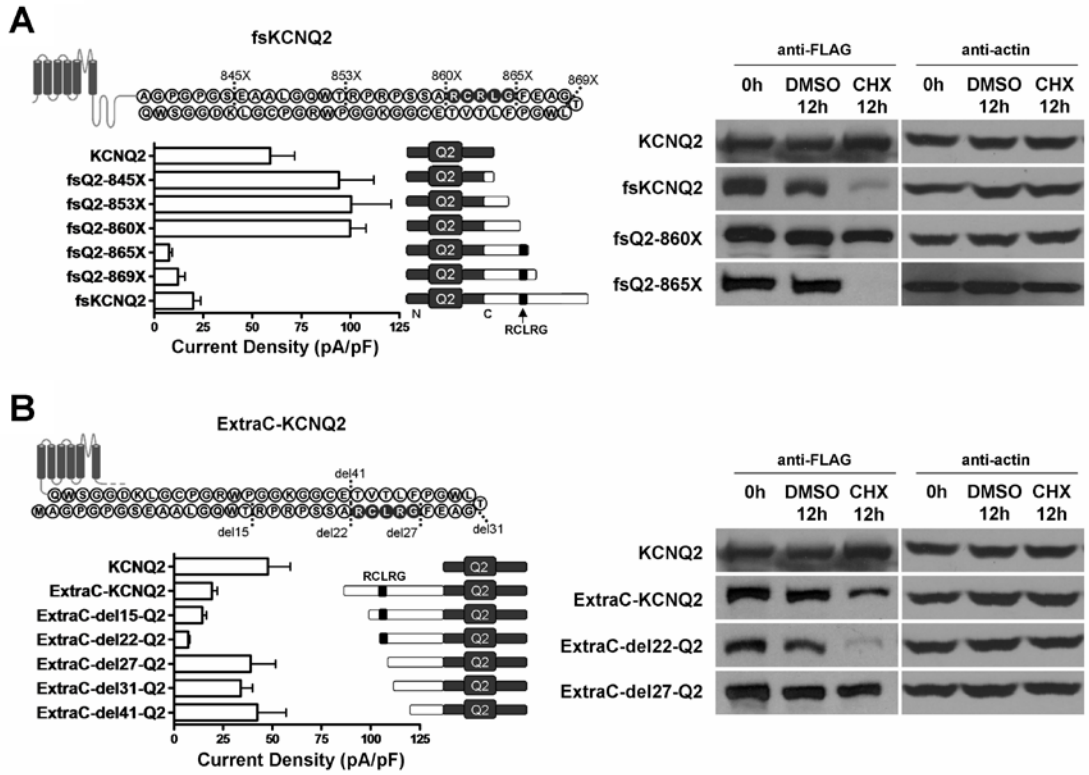

Figure 7